

See discussions, stats, and author profiles for this publication at:  
<https://www.researchgate.net/publication/28357833>

# Amorphous polymorphs in ice investigated by inelastic neutron scattering

ARTICLE *in* PHYSICA B CONDENSED MATTER · DECEMBER 1997

Impact Factor: 1.32 · DOI: 10.1016/S0921-4526(97)00749-7 · Source: OAI

---

CITATIONS

51

---

READS

8

6 AUTHORS, INCLUDING:



C. Austen Angell

Arizona State University

550 PUBLICATIONS 30,877 CITATIONS

SEE PROFILE



ELSEVIER

Physica B 241–243 (1998) 897–902

---

---

**PHYSICA B**

---

---

# Amorphous polymorphism in ice investigated by inelastic neutron scattering

H. Schober<sup>a,\*</sup>, M. Koza<sup>b</sup>, A. Tölle<sup>a</sup>, F. Fujara<sup>b</sup>, C.A. Angell<sup>c</sup>, R. Böhmer<sup>d</sup>

<sup>a</sup> *Institut Laue-Langevin, F-38042 Grenoble, France*

<sup>b</sup> *Fachbereich Physik, Universität Dortmund, D-44221 Dortmund, Germany*

<sup>c</sup> *Department of Chemistry, Arizona State University, Tempe, AZ 85287, USA*

<sup>d</sup> *Institut für Physikalische Chemie, Universität Mainz, D-55099 Mainz, Germany*

---

## Abstract

High-density  $I_{\text{hda}}$  and low-density  $I_{\text{lda}}$  amorphous ice phases have been investigated by inelastic neutron scattering (INS) with emphasis on the energy window from 0.5 to 20 meV. At variance with earlier measurements the spectra in the  $I_{\text{hda}}$  phase show a simple  $\omega^2$  behaviour in the acoustic region and the temperature dependence is found to be harmonic.  $I_{\text{hda}}$  converts with a strongly temperature-dependent rate towards  $I_{\text{lda}}$  ice. We have investigated in detail the time evolution of both the static and dynamic response functions at several temperatures. Elastic small-angle signals indicate the presence of strong heterogeneities at the early stages of the conversion process. At least two different time scales are present in the transition. The structural changes are reflected in the frequency distribution. The first peak in the phonon density-of-states softens appreciably when going from  $I_{\text{hda}}$  to  $I_{\text{lda}}$ . In the acoustic region there is evidence that  $I_{\text{lda}}$  is softer than both  $I_{\text{hda}}$  and crystalline cubic ice  $I_{\text{c}}$ . No signs of a fast ps process related to melting can be detected in the dynamics. © 1998 Elsevier Science B.V. All rights reserved.

PACS: 63.20 Dj; 64.60 My; 61.42.th

Keywords: Amorphous ice; Ice; Polymorphism

---

Water is a common liquid showing highly complex behaviour. During the last couple of years substantial efforts have been undertaken to establish the nature of the phase diagram in the supercooled region [1]. In this context the connection between the amorphous and liquid phases of water plays a central role. The existence of a line along

which the isothermal compressibility  $K_T$  is a maximum is established from molecular dynamics simulations [2]. Along this line  $K_T$  is found to increase with decreasing temperature. This does, however, not imply that  $K_T$  has to become singular [3]. The presence of a second critical point in the supercooled liquid region, inaccessible to experiment due to homogeneous nucleation of the crystalline phase, is therefore, from this point of view, still an open question. Only very recently direct

\* Corresponding author.

evidence for a first-order liquid–liquid phase transition in a model liquid has been obtained by extensive simulations [4].

If a first-order liquid–liquid transition line exists in real water then the two amorphous modifications of ice  $I_{\text{lda}}$  and  $I_{\text{hda}}$  may be considered the glassy forms of the respective low-density and high-density liquids. The mechanism of the non-symmetry breaking transition from  $I_{\text{hda}}$  to  $I_{\text{lda}}$  is interesting in its own right [5]. A direct link of this non-ergodic transition to the phase diagram of the equilibrium, undercooled liquid is certainly difficult to establish. There is nevertheless hope that the study of the transition will contribute important clues to the understanding of the liquid.

In this perspective we have undertaken a series of inelastic neutron scattering experiments (INS) using the cold-neutron time-of-flight instrument IN6 at the Institut Laue-Langevin in Grenoble (France) studying the amorphous ice phases and their transitions in much detail. In this context the high flux of the instrument IN6 is of particular importance as it allows us to follow the transitions in real time. This fact and the better energy resolution at low frequencies distinguishes our experiments from previous ones carried out on either three-axis [6] or thermal time-of-flight spectrometers [7]. Incident wavelengths of  $\lambda_i = 5.1$  and  $4.1 \text{ \AA}$  were employed to explore momentum transfers of  $Q_{\text{el}} = 0.3\text{--}2.0$  and  $1.2\text{--}2.6 \text{ \AA}^{-1}$  with elastic energy resolutions of  $\Delta E_{\text{el}} = 80$  and  $170 \text{ \mu eV}$ , respectively. All measurements were performed in energy gain mode.

After briefly presenting the experimental procedure used to produce  $I_{\text{hda}}$ , we will give a short description of the dynamics of the equilibrated phases before proceeding towards a discussion of the transformations.

$I_{\text{hda}}$  ( $\rho = 1.17 \pm 0.02 \text{ g/cm}^3$ ) was obtained by pressurizing hexagonal ice  $I_{\text{h}}$  at  $77 \text{ K}$  [8] beyond  $10 \text{ kbar}$  using a piston–cylinder apparatus similar to the one used by Bizid et al. [9]. The metastable compound was retrieved from the cell at ambient pressures crunched to powder and placed into a thin-walled aluminum container (1 mm hollow cylinder) which was then transferred from the liquid-nitrogen bath into the precooled cryostat. The sample chamber was held at  $80 \text{ K}$  and evacu-

ated. Due to the particular design of the container nitrogen initially trapped within the  $I_{\text{hda}}$  powder could be evacuated completely within about  $30 \text{ min}$ . This evacuation process was followed on-line by continuously recording INS spectra. During the actual experiment temperature stability was ensured by a small amount of helium exchange gas.

As we use the coherent scatterer  $\text{D}_2\text{O}$  contaminations with high-density crystalline ice phases become immediately obvious in the static structure factor  $S(Q)$  which is obtained by integration of  $S(Q, \omega)$  over  $\omega$  in the kinematically accessible region. Such contaminations were actually detected for seven out of 11 preparational runs, a fact already observed by other groups [9,10]. So far we are unable to link the presence of these phases to the preparational parameters like, e.g. cell diameter, compression speed or maximum attained pressure. Further investigations in this direction are under way. All the results presented here were obtained on pure samples.

In order to check upon anomalies and/or anharmonic behaviour, we investigated the frequency distribution of the equilibrated  $I_{\text{hda}}$  phase at  $20$  and  $80 \text{ K}$ . Fig. 1 shows the generalized density-of-states  $G(\omega)$  obtained from the time-of-flight spectra under the incoherent approximation [11] by integration over  $Q$ . No correction for multi-phonon processes was attempted, as the contributions are small at the temperatures and  $Q$ -values covered by

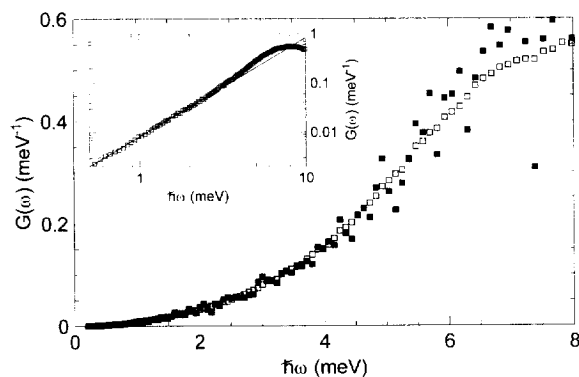


Fig. 1. Generalized density-of-states for  $I_{\text{hda}}$  at  $20 \text{ K}$  (full symbols) and  $80 \text{ K}$  (empty symbols). The system behaves harmonically. The spectra do not show significant signs of excess modes beyond  $\omega^2$  as shown by the inset.

the present experiment. The validity of the incoherent approximation was tested by comparison of  $G(\omega)$  as derived from both wavelengths. Besides resolution effects the results coincide.

The dynamic response of  $I_{\text{hda}}$  in the low-frequency region 0–10 meV is obviously harmonic between 20 and 80 K. This is in agreement with molecular dynamics calculations [12] which predict only a very small number of unstable modes in  $I_{\text{hda}}$  at low temperatures. The result is, on the other hand, at variance with earlier experiments [13] on protonated  $I_{\text{hda}}$  reporting  $T$ -dependent anomalies in the energy range from 1.6 to 2.4 meV. It has to be noted that we would be unable to detect hypothetical anomalies confined to the  $Q$  range outside our experimental window, i.e.  $0.3 \text{ \AA} < Q < 2.6 \text{ \AA}$ .

In contrast to most other amorphous materials we do not find signatures of excess modes (Boson peak) at low frequencies over the crystalline hexagonal  $I_{\text{h}}$  and cubic  $I_{\text{c}}$  counterparts. As demonstrated in the inset of Fig. 1,  $G(\omega)$  can be well described by a  $\omega^2$  law, as expected for acoustic modes, up to about 4 meV. The fact that  $G(\omega)$  for  $I_{\text{hda}}$  and  $I_{\text{c}}/I_{\text{h}}$  nearly coincide (see Fig. 2) for  $\hbar\omega < 4 \text{ meV}$  to us comes as a surprise. It seems that the softening of the acoustic modes expected from the distortion of the hydrogen-bond network of  $I_{\text{hda}}$  is compensated by the drastic increase in density. These observations have, however, to be confirmed by inelastic X-ray experiments as small deviations of the actual density-of-states from the experimental result based on the incoherent approximation cannot be excluded.

The vibrational spectra of  $I_{\text{hda}}$  and  $I_{\text{lda}}$  (obtained by annealing  $I_{\text{hda}}$  at 127 K) are markedly different as shown in Fig. 2. The main peak of the translational band situated at about 8 meV in  $I_{\text{hda}}$  sharpens and shifts down to 6 meV in  $I_{\text{lda}}$ . The plateau between 12 and 30 meV becomes more structured and the librational band moves to higher frequencies as already observed by Klug et al. [6]. In general, above 4 meV, the  $I_{\text{lda}}$  translational spectrum compares very favourably with the one of cubic crystalline ice  $I_{\text{c}}$ . Besides a main peak at 6 meV a shoulder at about 8 meV and two dips at 14 and 22 meV are present in both ice modifications. This may be explained by the fact that modes with optic character are sensitive primarily to the

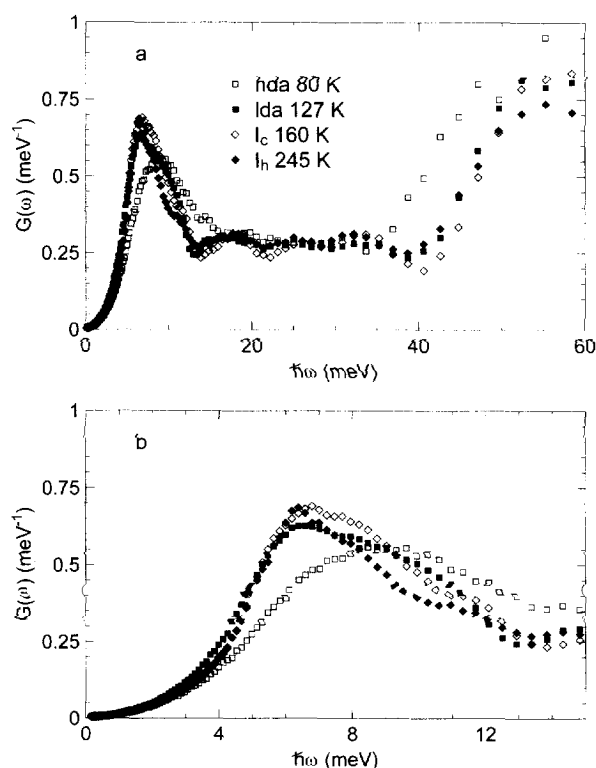


Fig. 2. Comparison of the generalized density-of-states for  $I_{\text{hda}}$ ,  $I_{\text{lda}}$ ,  $I_{\text{c}}$  and  $I_{\text{h}}$  ice.

direct molecular environment. This environment should be similar in  $I_{\text{c}}$  and  $I_{\text{lda}}$  due to the resaturation of the hydrogen-bond network. In  $I_{\text{hda}}$  this network is highly perturbed leading to a larger distribution of possible nearest-neighbour configurations which in turn may provoke a broadening of the peaks in the optic region. In the very low-frequency region ( $\hbar\omega < 5 \text{ meV}$ ) the  $I_{\text{lda}}$  density-of-states systematically exceeds the one of the other phases. This excess does not lead to a clear shoulder in the density-of-states which could be directly interpreted as a Boson peak but the data follow as in  $I_{\text{hda}}$  to a good approximation a  $\omega^2$  law.

The static structure factor  $S(Q)$  of  $I_{\text{hda}}$  is found to be invariant on the time scale of hours up to temperatures slightly above 80 K. For higher temperatures,  $S(Q)$  evolves with a temperature-dependent rate signalling the onset of the transformation towards  $I_{\text{lda}}$ . We have followed this transition for two

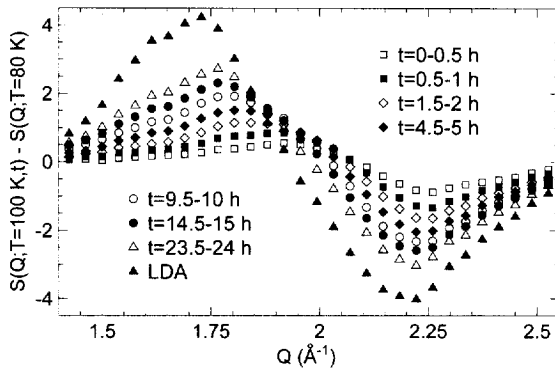


Fig. 3. Time evolution of  $S_{\text{diff}}(Q; T = 100 \text{ K})$  as defined in Eq. (1).

temperatures  $T = 100$  and  $103 \text{ K}$  using an incident wavelength of  $4.1 \text{ Å}$ . At these temperatures the evolution of  $S(Q, \omega)$  is slow enough to be followed in detail despite accumulation times of 30 min necessary to obtain reasonable data statistics.

In Fig. 3 we show the relative change

$$S_{\text{diff}}(Q; T, t) := S(Q; T, t) - S(Q; T = 80 \text{ K}) \quad (1)$$

for the  $100 \text{ K}$  run at selected times  $t$ . Assuming a simple nucleation and growth scenario of  $I_{\text{lda}}$  domains in a  $I_{\text{hda}}$  matrix leads to

$$S_{\text{diff}}(Q; T, t) = a(T, t)(S_{\text{lda}}(Q) - S_{\text{hda}}(Q)), \quad (2)$$

apart from the small-angle region corresponding to the size of the nucleation clusters. The temperature and time dependence of  $S_{\text{diff}}(Q; T, t)$  is contained in the  $Q$ -independent prefactor  $a(T, t)$  which measures the fraction of material present in the form of  $I_{\text{lda}}$  domains implying that the line shape of  $S_{\text{diff}}(Q; T, t)$  is conserved.

It is already realized in Fig. 3 that the line shape of  $S_{\text{diff}}(Q; T)$  is not conserved. The line-shape variations become even more obvious in Fig. 4 where we present  $S_{\text{diff}}(Q; T = 100 \text{ K}, t)$  as a function of  $t$ . The functional form of  $S_{\text{diff}}(Q; T = 100 \text{ K}, t)$  is clearly distinct for different  $Q$ .

To obtain numerical information on the time scales involved in the transformation process we fitted the data to exponential growth laws. It turns out that at least two growth constants are neces-

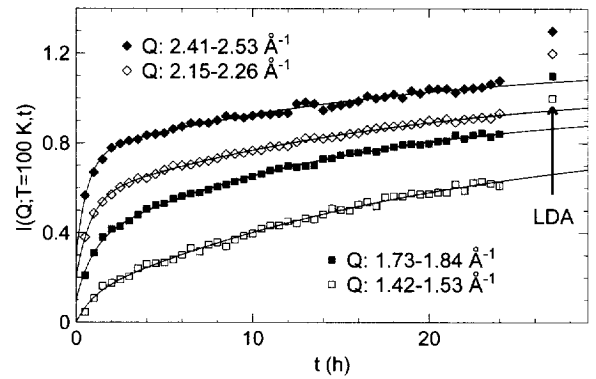


Fig. 4. Functional dependence upon time of the static structure factor for selected ranges of  $Q$  during the transition at  $100 \text{ K}$ . The data are expressed in units of  $S_{\text{lda}}(Q) - S_{\text{hda}}(Q)$  and shifted relative to each other by  $0.1$ . Lines are fits to the data according to Eq. (3).

sary to obtain a satisfying data description:

$$S_{\text{diff}}(Q; T, t) = a_Q(1 - (b_Q e^{-t/\tau_1} + c_Q e^{-t/\tau_2})),$$

$$b_Q + c_Q = 1. \quad (3)$$

A Kohlrausch–Williams–Watt (KWW) function

$$f(t) = a_Q(1 - e^{(-t/\tau_Q)^{\beta_Q}}) \quad (4)$$

which is synonymous to a distribution of time scales yields a poorer data reproduction. The line-shape variation as a function of time mentioned above translates into the  $Q$ -dependence of the fit-parameters given in Table 1. At  $103 \text{ K}$  the situation is less clear as KWW and two-exponential fits give similar descriptions.

Due to the use of a flat container in reflection geometry, the small-angle part of the detector bank

Table 1

Parameters obtained by fitting Eq. (3) to  $S_{\text{diff}}(Q; T = 100 \text{ K})$  as defined in Eq. (1). The value of  $a$  expressed in units of  $(S_{\text{lda}}(Q) - S_{\text{hda}}(Q))$  has been assumed  $Q$ -independent. Allowing for a  $Q$  dependence of  $a$  does not improve the quality of the fit

$Q$ (Å <sup>-1</sup> )	$a$	$b$	$\tau_1$ (h)	$\tau_2$ (h)
1.42–1.53	0.87	0.9	20.8	0.9
1.73–1.84	0.87	0.7	15.3	0.9
2.15–2.26	0.87	0.6	18.9	0.8
2.41–2.53	0.87	0.5	18.5	0.7

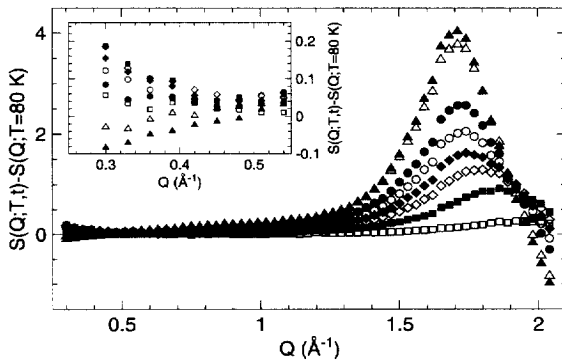


Fig. 5. Evolution of  $S_{\text{diff}}(Q;T)$  (for definition see Eq. (1)) as a function of time and temperature. The inset shows the small-angle part. The negative values for  $I_{\text{da}}$  are consistent with the fact that  $S(Q;T) \rightarrow nk_b T \chi_T$  for  $q \rightarrow 0$ . Open squares: 90 K; full squares: 105 K first hour; open diamonds: 105 K second hour; full diamonds: 105 K third hour; open circles: 105 K sixth hour; full circles: 111 K first 30 min; open triangles: 117 K first 30 min; full triangles: 127 K first 30 min.

was hidden for the 100 and 103 K runs. This region had already been investigated for somewhat different temperatures in an earlier experiment using 5.12 Å neutrons and a cylindrical sample geometry. Transient small-angle signals  $Q < 0.5 \text{ Å}^{-1}$  (see Fig. 5) were observed at the early stages of the transformation process (90–127 K).

The experimental information may be summarized as follows: the strong  $Q$ -variation of the parameters governing the faster process makes it difficult to associate it with the nucleation of  $I_{\text{lda}}$ -type clusters, although strong heterogeneities are definitely present at this state of the conversion. The fact that the nucleated clusters are different from relaxed  $I_{\text{lda}}$  and structurally evolve with time can be understood on the basis of the strong volume changes associated with the transformation. For homogeneous nucleation, i.e. in the absence of free volume, this leads to internal pressures which influences the structural properties of the nucleated clusters. The atomic arrangement simply cannot be expected to be of the relaxed  $I_{\text{lda}}$ -type at ambient pressure. In addition, the internal pressure which also acts on the host  $I_{\text{hda}}$  matrix may slow down the transformation kinetics in a complex way. A detailed study of the  $I_{\text{lda}}$  structure factor over a broad  $Q$ -range as a function of external pressure will

allow us to evaluate the effects of internal pressure on the transformation process more quantitatively.

In a standard scenario, the slower process might be associated with a simple growth or relaxation process. In this context, it is instructive to note that the fit parameter  $a(Q)$  if expressed in units of the final  $I_{\text{lda}}$  structure factor, i.e.  $a(Q)/(S_{\text{lda}}(Q) - S_{\text{lda}}(Q))$  can be assumed  $Q$  independent but is not equal to one.  $S_{\text{lda}}(Q)$  is determined after equilibration at 127 K. This fact indicates that the process at 100 K does not lead to a fully relaxed  $I_{\text{lda}}$  state, at least on the time scales explored by the present experiment. The transformation from  $I_{\text{hda}}$  to  $I_{\text{lda}}$ , therefore, proceeds via the exploration of some well-developed intermediate basin within the energy landscape of amorphous ice.

One may expect further insight into the transition mechanism from the study of the frequency distributions. If the transition were driven by strong anharmonicities within the  $I_{\text{hda}}$  phase the superposition principle should be violated as long as  $I_{\text{hda}}$  is present in the system. This is not the case. For longer times ( $> 6$  h at 100 K) the dynamical response for the intermediate stages of the conversion process can to a high degree of accuracy be expressed as a superposition of  $I_{\text{lda}}$  and  $I_{\text{hda}}$  ( $T = 80$  K) response functions. This is, in particular, the case for the region 8–15 meV, which according to molecular dynamics calculations [14] plays an important role in the transition from  $I_{\text{h}}$  to  $I_{\text{hda}}$ . As can be seen from Fig. 6, a slight violation of the superposition principle cannot be excluded for the shorter times. Such a superposition would actually not be expected given the complex evolution of the static structure factor. Better statistics, i.e. measurements at even lower transformation temperatures, will be needed to give a definite answer to the question.

No quasi-elastic signals indicative of statistical particle movement are observed in our spectra. This applies in particular to the  $I_{\text{lda}} \rightarrow I_{\text{c}}$  transformation process which lasted for several hours at  $137 \text{ K} < T < 160 \text{ K}$ . Therefore, if a melting process precedes the transitions [15] the corresponding relaxation rates in the liquid must either be slow on the ps time scale (absence of fast process) or the corresponding liquid state extremely short-lived compared to the data accumulation time of hours.

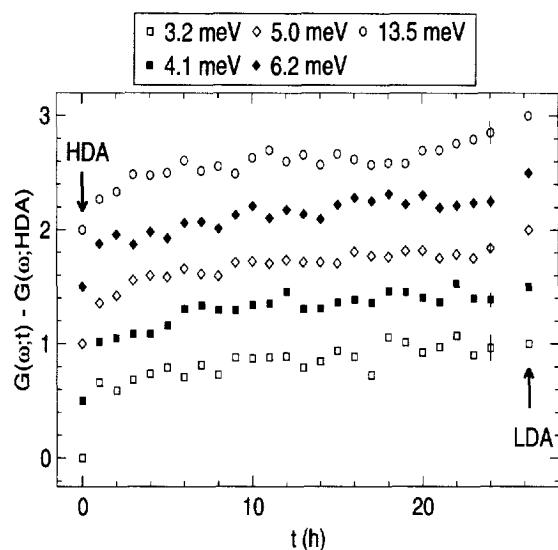


Fig. 6. Time evolution of the generalized density of states for selected energies at 100 K. Open circles: 13.5 meV; closed diamonds: 6.2 meV; open diamonds: 5.0 meV; closed squares: 4.1 meV; open squares: 3.2 meV. Shown are the absolute differences with respect to the original  $I_{\text{hda}}$  spectrum.

INS experiments have been used to investigate the properties of amorphous ice modifications. The  $I_{\text{hda}}$  modification is found to behave like a normal harmonic solid. Excess modes at low frequencies encountered in most other amorphous materials are absent in  $I_{\text{hda}}$  within the  $Q$  range investigated. The perturbed hydrogen-bond network [14] is reflected in a strong redistribution of spectral weights.  $I_{\text{lda}}$  has a restored hydrogen-bond network and the spectra resemble in most aspects the crystalline phases. Excess modes in  $I_{\text{lda}}$  cannot be generally excluded. However, if present, they do not lead to a clear shoulder in the density-of-states and are, therefore, difficult to distinguish from a softening of the sound-wave spectrum. Inelastic X-ray experiments will be necessary to separate the two scenarios. There is strong structural evidence for the existence of amorphous states which might be termed intermediate to  $I_{\text{hda}}$  and  $I_{\text{lda}}$ . These states are generated during the transformation process. Transient at the formation temperature they can be frozen into metastable states by fast cooling. The

degree of heterogeneity of these states varies with the thermal history and has to be studied in further detail using small-angle scattering. As there is no broken symmetry between amorphous phases, a classification relies on clear thermodynamic phase boundaries. In contrast to the liquid–gas or liquid–liquid cases it is difficult to establish such a boundary for amorphous–amorphous systems which are by definition in the glassy state, i.e. out of thermal equilibrium. Therefore, the present experiment is unable to discriminate between (i) a continuous transition from high-density towards low-density ice forms crossing a line of compressibility maxima and (ii) a kinetically slowed down first-order transition in a two-state coexistence region.

## References

- [1] P.H. Poole, F. Sciortino, U. Essmann, H.E. Stanley, *Nature* 360 (1992) 324.
- [2] F. Sciortino, P.H. Poole, U. Essmann, H.E. Stanley, *Phys. Rev. E* 55 (1997) 727.
- [3] S. Sastry, P.G. Debenedetti, F. Sciortino, H.E. Stanley, *Phys. Rev. E* 53 (1996) 6144.
- [4] S. Harrington, R. Zhang, P.H. Poole, F. Sciortino, H.E. Stanley, *Phys. Rev. Lett.* 78 (1997) 2409.
- [5] P.H. Poole, T. Grande, C.A. Angell, P.F. McMillan, *Science* 275 (1997) 322.
- [6] D.D. Klug, E. Whalley, E.C. Svensson, J.H. Root, V.F. Sears, *Phys. Rev. B* 44 (1994) 841.
- [7] A.I. Kolesnikov, V.V. Sinitsyn, E.G. Ponyatovsky, I. Natanek, L.S. Smirnov, *J. Phys.: Condens. Matter* 6 (1994) 375.
- [8] O. Mishima, L.D. Calvert, E. Whalley, *Nature* 310 (1984) 393.
- [9] A. Bizid, L. Bosio, A. Defrain, M. Oumezzine, *J. Chem. Phys.* 87 (1987) 2225.
- [10] M.C. Bellisent-Funel, J. Teixeira, L. Bosio, *J. Chem. Phys.* 87 (1987) 2231; L. Bosio, G.P. Johari, J. Teixeira, *Phys. Rev. Lett.* 56 (1986) 460.
- [11] S.N. Taraskin, S.R. Elliot, *Phys. Rev. B* 55 (1997) 117.
- [12] T. Okabe, H. Tanaka, K. Nakanishi, *Phys. Rev. E* 53 (1996) 2638.
- [13] E.C. Svensson, W. Montfrooij, V.F. Sears, D.D. Klug, *Physica B* 194–196 (1994) 409.
- [14] J.S. Tse, *J. Chem. Phys.* 96 (1992) 5482.
- [15] Y.P. Handa, O. Mishima, E. Whalley, *J. Chem. Phys.* 84 (1986) 2766; Y.P. Handa, D.D. Klug, *J. Chem. Phys.* 92 (1988) 3323; A. Hallbrucker, E. Mayer, G.P. Johari, *Philos. Mag. B* 60 (1989) 179; G.P. Johari, *J. Chem. Phys.* 102 (1995) 6224.